Temperature enhanced mcr-1 colistin resistance gene detection with electrochemical impedance spectroscopy biosensors

Temperature enhanced mcr-1 colistin resistance gene detection with electrochemical impedance spectroscopy biosensors

Journal:	*Analytical Chemistry*
Manuscript ID	ac-2020-006665.R2
Manuscript Type:	Article
Date Submitted by the Author:	19-Mar-2021
Complete List of Authors:	Schulze, Holger; The University of Edinburgh, Infection Medicine, Edinburgh Medical School, College of Medicine and Veterinary Medicine Arnott, Andrew; The University of Edinburgh, Infection Medicine, Edinburgh Medical School, College of Medicine and Veterinary Medicine Libori, Adriana; The University of Edinburgh Edinburgh Medical School, Infection Medicine Obaje, Eleojo; The University of Edinburgh, Infection Medicine, Edinburgh Medical School, College of Medicine and Veterinary Medicine Bachmann, Till T.; The University of Edinburgh, Infection Medicine, Edinburgh Medical School, College of Medicine and Veterinary Medicine

Temperature enhanced *mcr-1* colistin resistance gene detection with electrochemical impedance spectroscopy biosensors

*Holger Schulze, Andrew Arnott, Adriana Libori, Eleojo A. Obaje, Till T. Bachmann**

Infection Medicine, Edinburgh Medical School, College of Medicine and Veterinary Medicine, The University of Edinburgh, Chancellor's Building, 49 Little France Crescent, Edinburgh EH16 4SB, Scotland, UK.

* Corresponding author: phone: +44 131 242 9437, email: Till.Bachmann@ed.ac.uk

Abstract

Antibiotic resistance is now one of the biggest threats humankind is facing as highlighted in a declaration by the General Assembly of the United Nations in 2016. Especially, the growing resistance rates of Gram-negative bacteria causes increasing concerns. The occurrence of the easily transferable, plasmid-encoded *mcr-1* colistin resistance gene further worsened the situation significantly enhancing the risk of the occurrence of pan-resistant bacteria. There is therefore a strong demand for new rapid molecular diagnostic tests for the detection of *mcr-1* gene associated colistin resistance. Electrochemical impedance spectroscopy (EIS) is a well-suited method for rapid antimicrobial resistance detection as it enables rapid, label-free target detection in a cost efficient manner. Here, we describe the development of an EIS-based *mcr-1* gene detection test, including the design of *mcr-1* specific peptide nucleic acid probes and assay specificity optimisation through temperature-controlled real-time kinetic EIS measurements. A new flow cell measurement set-up enabled for the first time detailed real-time, kinetic temperature-controlled hybridisation and de-hybridisation studies of EIS-based nucleic acid biosensors. The temperature-controlled EIS set-up allowed single nucleotide polymorphism (SNP) discrimination. Target hybridisation at 60 °C enhanced the perfect match/mismatch (PM/MM) discrimination ratio from 2.1 at room temperature to 3.4. A hybridisation and washing temperature of 55 °C further increased the PM/MM discrimination ratio to 5.7 by diminishing the mismatch signal during the wash step while keeping the perfect match signal. This newly developed *mcr-1* gene detection test enabled the direct, specific label and amplification-free detection of *mcr-1* gene harbouring plasmids from *Escherichia coli*.

Keywords

Electrochemical impedance spectroscopy, single-nucleotide polymorphism (SNP) discrimination, peptide nucleic acid, *mcr-1*, colistin resistance, antimicrobial resistance (AMR) diagnostics

1 Introduction

Antimicrobial resistance (AMR), and here especially the resistance of bacteria to antibiotic treatment, is one of the biggest threats humankind is facing in the 21st century. The recently published review on antimicrobial resistance chaired by Jim O'Neill has predicted that AMR could cause an additional 10 million deaths per year and a loss of up to US$100 trillion from global GDP by 2050 if no immediate actions are taken now.[1] Leading international organisations including the World Health Organisation (WHO), the European Centre for Disease Prevention and Control (ECDC), the US Centers for Disease Control and Prevention (CDC) as well as the European Commission and many national governments identified this as an urgent problem, which demands immediate action. On the 21st of September 2016, world leaders from all 193 member states signed a declaration to combat the proliferation of antibiotic resistance during the General Assembly of the United Nations in New York. Today, the FAO/OIE/WHO Tripartite Joint Secretariat on Antimicrobial Resistance is the global lead to tackle AMR from a One Health perspective.

Especially, the growing resistance of Gram-negative bacteria is a major threat for human health. Carbapenem-resistant *Enterobacteriaceae*, *Acinetobacter baumannii*, and *Pseudomonas aeruginosa* have been identified as the most critical bacteria in a global WHO priority pathogen list for R&D of new antibiotics.[2] Colistin (polymyxin E) and polymyxin B are increasingly used as the last-resort antibiotics to treat carbapenem-resistant Gram-negative bacteria. Until recently, it has been thought that polymyxin resistance is merely caused by various chromosomal mutations of Gram-negative bacteria and not by resistance genes on transferrable mobile elements like plasmids, which can easily spread between pathogens.[3] In 2015, the first plasmid-encoded, transferable colistin resistance mechanism encoded by the *mcr-1* gene has been detected on a plasmid in an *Escherichia coli* strain in China by Liu et al and has now been found in more than 30 countries around the world across five continents in samples of animal, environmental and human origin.[4,5] The existence of these transferable colistin-resistance genes is increasing the risk of us entering a *'post-antibiotic era'* in which the ability to treat infections that once were believed to be under control will be at risk again. There are already first reports of almost untreatable pathogens, which carried the *mcr-1* gene together with various carbapenem-

resistance genes like the New Delhi Metallo-beta-lactamase (NDM) and *Klebsiella pneumoniae carbapenemases* (KPCs) genes.[5–8] The co-existence of colistin and carbapenem-resistance is associated with high in-hospital mortality rates of 69-75 % in Greece and India.[9,10] Up to now there are six known variants of the *mcr-1* gene, *mcr-1.2* [11] (GenBank accession no. KX236309), *mcr-1.3* (NG_052861), *mcr-1.4* (KY041856), *mcr-1.5* (KY283125), *mcr-1.6* [12] (NG_052893), and *mcr-1.7* (KY488488), which only differ in one or two nucleotides from the *mcr-1* gene. Shortly after the identification of the *mcr-1* gene a novel colistin resistance gene, *mcr-2*, has been found by Xavier et al. in *Escherichia coli* strains recovered from piglets in Belgium.[13] The *mcr-2* gene shares 77% nucleotide and 81 % amino acid identity with *mcr-1*. Recently, a novel *mcr-3* gene has been identified in colistin-resistant *Escherichia coli* in faecal samples from a pig farm in China. The *mcr-3* gene showed 45 % and 47 % nucleotide sequence identity to the *mcr-1* and *mcr-2* gene, respectively.[14] Until now, nine different variants of the *mcr* gene have been identified with the *mcr-9* gene first described in 2019 in a multidrug-resistant *Salmonella enterica* strain isolated from a human patient in Washington State in 2010.[15,16]

Rapid diagnostics have been identified as one of the key measures to reduce the misuse of antibiotics in up to now still mainly empiric treatment regimens to support therapy decision and the selection of the right antibiotic.[17,18] Current standard methods, which are mainly culture-based, are too slow and lack information depth to enable such tailored therapy decisions. One of the main recommendations of the review on antimicrobial resistance chaired by Jim O'Neill was that "[rich countries] should make it mandatory that by 2020 the prescription of antibiotics will need to be informed by data and testing technology wherever available and effective in informing the doctor's judgement to prescribe".[1]

In recent years, various biosensor tests and here especially electrochemical biosensors have been developed for AMR diagnostics.[19–24] Electrochemical impedance spectroscopy (EIS) is a label-free detection method which has been applied for various different types of targets ranging from entire bacteria, over nucleic acid targets to proteins and small molecules.[25,26,35,27–34] We have previously developed assays for the detection of the *mecA* gene and genomic DNA of methicillin-resistant *S. aureus* (MRSA), the New Delhi Metallo-beta-lactamase (NDM) carbapenem-resistance gene and for bacterial 16S ribosomal RNA for species identification.[36–39] This assay portfolio was complemented

with tests for the host protein infection biomarkers TREM-1 and MMP9 and homoserine lactone bacterial quorum sensing molecules.[40]

In this paper, we increased the target spectrum of our EIS platform to cover the *mcr-1* gene by designing new *mcr-1* specific peptide nucleic acid (PNA) probes and testing its capability to discriminate fully complementary targets from single nucleotide mismatch targets at room temperature and at various different hybridisation temperatures. We evaluated the optimal hybridisation temperature to achieve the highest degree of specificity and derived binding and de-binding kinetics from continuous kinetic EIS measurements at different hybridisation temperatures.

2 Materials and methods

2.1 Materials and reagents

PNA oligonucleotides were ordered via Cambridge Research Biochemicals (Cleveland, UK) from Panagene (Daejeon, South Korea). DNA oligonucleotides were purchased from Metabion (Martinsried, Germany). Tris(2-carboxyethyl)phosphine hydrochloride (TCEP), potassium hexacyanoferrate(III), potassium hexacyanoferrate(II) trihydrate, sodium dihydrogen phosphate, disodium hydrogen phosphate, iron(III) chloride, potassium chloride, and dimethyl sulfoxide (DMSO) were purchased from Sigma Aldrich (Poole, UK). Mercaptohexanol (MCH) has been received from ProChimia Surfaces Sp. (Sopot, Poland). Deionised water was used throughout the study (>18 MΩ cm). DropSens (Oviedo, Spain) screen-printed gold electrodes DRP-C223BT with a 1.6 mm gold working electrode, a gold counter and silver reference electrode were bought from Metrohm UK (Runcorn, UK). The EIS measurement cell for temperature controlled EIS measurements were obtained from MiniFAB (Melbourne, Australia). The *E. coli mcr-1* reference strain NCTC 13846 was obtained from Public Health England culture collection, London, UK. The *E. coli* NDM-1 reference strain ATCC BAA-2452 was received from ATCC, Manassas, Virginia, U.S.A.

2.2 Probe design

Mcr-1 specific probes of 20 nt in length were designed in silico with an online tool named UPS Unique Probe Selector (http://array.iis.sinica.edu.tw/ups/).[41] The UPS algorithm considers "GC content, the secondary structure, melting temperature (T_m), the stability of the probe-target duplex estimated by the thermodynamic model, sequence complexity, similarity of probes to non-target sequences, and other empirical parameters used in the laboratory" when selecting probes. The option to select probes at a 'pangenomic level' was selected and the 1626 bp *mcr-1* gene sequence (accession no. KP347127.1: 22413-24038, *Escherichia coli* strain SHP45 plasmid pHNSHP45) was entered in FASTA format. A salt concentration of 0.33 M was specified and subsequently 10 probes, 20 nucleotides in length were generated.

Pairwise nucleotide sequence alignments of the *mcr-1* gene with the *mcr-1* variant genes and the *mcr-2* gene and the *mcr* PNA probes with the *mcr-1* and *mcr-2* genes were performed with the EMBOSS Water algorithm, which uses the Smith-Waterman algorithm. The alignment tool was accessed through the European Bioinformatics Institute (EMBL-EBI) website (https://www.ebi.ac.uk/Tools/psa/emboss_water/, accessed 28 December 2020) with the following standard settings: program: water version: 6.6.0/matrix: EDNAFULL/gapopen: 10.0/gapext: 0.5/format: pair/stype: dna. The candidate *mcr-1* PNA probes were checked for PNA specific design criteria with the PNA from PNA Bio (Newbury Park, USA) (https://www.pnabio.com/support/PNA_Tool.htm, accessed 28 December 2020) and with the PNA Probe Designer tool from Life Technologies (Carlsbad, USA).

2.3 Bacteria culture and plasmid DNA extraction

Mcr-1 and NDM-1 plasmids were extracted from a 100 mL Luria-Bertani (LB) broth culture of the *E. coli* reference strains NCTC 13846 and ATCC BAA-2452, respectively. Qiagen plasmid midi kits using Qiagen-Tip gravity flow anion-exchange columns (Qiagen, Hilden, Germany) were used for plasmid extraction. The 100 mL LB broth *E. coli* strains were cultivated for 16h at 37 ^{0}C at 200 rpm in an Infors shaking incubator (Infors HT, Bottmingen-Basel, Switzerland). *Mcr-1* and NMD-1 plasmid DNA was dissolved in 1x EIS buffer (0.2 mM $K_4[Fe(CN)_6]$ + 0.2 mM $K_3[Fe(CN)_6]$ + 10 mM phosphate buffer + 20 mM NaCl, pH 7) and heat denatured for 5 min at 95 ^{0}C, followed by 3 min incubation at 65 ^{0}C before adding the plasmid solution onto the functionalised electrodes in the flow cells (MiniFAB, Melbourne, Australia).

2.4 Electrode preparation

Screen-printed DropSens DRP-C223BT 1.6 mm gold working electrode sensors were used for all tests. The silver reference electrode were transferred into a Ag/AgCl quasi reference electrode by incubating the silver electrode with a 50 mM aqueous $FeCl_3$ solution for 20 s, followed by rinsing with water and drying under Argon gas. The electrodes were cleaned using cyclic voltammetry in 100 mM aqueous

sulphuric acid solution applying ten CV cycles between 0 - 1.6V and three cycles between 0 - 1.3V. After cleaning, the gold working electrodes were incubated with 5 µL of a solution of 1.5 µM thiol-modified PNA solution + 30 µM MCH + 5 mM TCEP in 50% (v/v) DMSO for 16 h at room temperature (RT) in a humidification chamber at around 75 % humidity, generated by a saturated potassium chloride solution in the chamber. Electrodes were rinsed in 50% (v/v) DMSO and all three electrodes were incubated with 50 µL of a solution of 1 mM MCH + 5 mM TCEP in 50% (v/v) DMSO for 1h at RT in the humidification chamber. After blocking with MCH electrodes were washed with 3x 1 mL 50% (v/v) DMSO and then with water.

2.5 EIS measurements

Functionalised electrodes were transferred into MiniFAB flow cells (Melbourne, Australia) on a preheated Stuart SD160 Digital Hotplate (Keison Products, Chelmsford, UK) attached to an Metrohm Autolab Potentiostat Galvanostat, PGSTAT128N (Utrecht, Netherlands). The potentiostat was controlled by Nova 2 software at open circuit potential at an amplitude of 10 mV rms at 20 frequencies in the range 100 000 Hz – 0.3 Hz. The required hot plate temperatures for a certain solution temperature inside the measurement cell are listed in Table S2 in the supplementary file. For each run, four sensors were connected to the potentiostat via a MUX MULTI 4 multiplexing module and tested sequentially. The time duration of one EIS spectrum including OCP measurement was 70 s, which resulted in a measurement interval of 4.7 min for each of the four sensors. Kinetic EIS measurements were performed in 0.2 mM $K_4[Fe(CN)_6]$ + 0.2 mM $K_3[Fe(CN)_6]$ + 10 mM phosphate buffer + 20 mM NaCl, pH 7. The sample volume inside the measurement cell was 50 µL. The EIS buffer without target for baseline measurements and with target DNA oligonucleotides for hybridisation detection were pre-incubated for 5 min 15°C degrees higher than the desired experimental temperature in an Eppendorf Thermomixer Comfort (Hamburg, Germany). Following three baseline EIS measurements on each of the four electrodes the solution was replaced with measurement buffer containing target DNA oligonucleotides. The flow cells were covered with sterile tape to prevent evaporation during the test.

3 Results and discussion

3.1 Mcr-1 PNA probe design

A set of ten 20 nucleotide long *mcr-1* specific PNA probes have been *in-silico* designed with an online tool named UPS Unique Probe Selector to specifically detect the *mcr-1* colistin resistance gene (see Table 1*)*. The candidate probes were also checked for PNA probe specific design criteria, which are that the purine content should be below 60%, the maximum purine stretch to be four in a row, and the maximum number of guanine residues to be three in a row. The ten newly designed *mcr-1* specific PNA probes cover the whole range of the 1.6 kb long *mcr-1* gene, from probe #10, which is complementary to nucleotides 32 to 51 of the *mcr-1* gene, to probe #7 at position 1489 - 1508. All of these ten PNA probes are also fully complementary to the six recently identified variants of the *mcr-1* gene, *mcr-1.2* (GenBank accession no. KX236309), *mcr-1.3* (NG_052861), *mcr-1.4* (KY041856), *mcr-1.5* (KY283125), *mcr-1.6*(Lu et al. 2017) (NG_052893), and *mcr-1.7* (KY488488) and will therefore also detect these *mcr-1* variants. The *mcr-1.2*, *mcr-1.4*, *mcr-1.5*, and *mcr-1.7* genes differ from *mcr-1* in just one single nucleotide polymorphism (SNP) at position 8, 1318, 1354, and 643, respectively. The *mcr-1.3* gene differs from *mcr-1* at position 111 and 112 and the *mcr-1.6* gene has two SNPs at position 1263 and 1607. The *mcr-2* gene shares 77 % nucleotide identity with *mcr-1*. The ten *mcr-1* specific PNA probes vary in their identity towards the *mcr-2* gene. Probe #5 is also fully complementary to the *mcr-2* gene and will therefore cover both the *mcr-1* and *mcr-2* gene. Other probes show reduced complementarity to the *mcr-2* gene ranging from 95 % identity to only 60 % identity towards the *mcr-2* gene. *Mcr-1* probe #1 has an 80% complementarity towards the *mcr-2* gene with a stretch of nine complementary nucleotides. The theoretical melting temperature of this nine nucleotide long PNA/DNA stretch calculated with the Life Technologies PNA Probe Designer online tool is 44 °C for 1 µM target concentration, 27 °C for 1 nM target, and below 20 °C for 1 pM target, respectively.

Insert Table 1 here

3.2 Electrochemical impedance spectroscopy-based mcr-1 PNA probe characterisation at room temperature

From the list of *mcr-1* candidate probes probe 1, which binds to the 1.6 kb long *mcr-1* gene between nucleotide position 1107 and 1126, was selected for EIS-based evaluation. This PNA probe was immobilised on gold screen-printed electrodes via a 3.8 nm long C11M-AEEEA (HS-$(CH_2)_{11}$-$(CH_2CH_2O)_3$) spacer with a terminal thiol group in a mixed monolayer consisting of the thiol-modified PNA probe and mercaptohexanol to form a stable probe layer and prevent unspecific adsorption for example of non-complementary target molecules. Tris(2-carboxyethyl)phosphine hydrochloride (TCEP) was added to the probe solution to cleave any existing disulphide bonds of mercaptohexanol molecules and thiol-modified PNA probes and thus provide full reactivity of monomeric mercaptohexanol and PNA probes for the gold-thiol bond formation on the electrode surface. The principle of the temperature controlled, label-free EIS-based detection of plasmid encoded antibiotic resistance genes is depicted in Scheme 1. Figure 1 shows kinetic EIS data obtained from testing the *mcr-1* probe 1 with a fully complementary target, a target with a single nucleotide mismatch and a non-complementary NDM-1 target at 20 °C. EIS measurements were performed continuously during the incubation with the target solutions (1 µM) and EIS buffer (negative control), respectively. The hybridisation of the fully complementary target to the immobilised probe caused a rapid increase of the charge transfer resistance (Rct) over time. Whereas, incubation with the same concentration of a NDM-1 target sequence, which is non-complementary to the probe sequence or respectively has only a three base-pair long stretch of complementary bases resulted in no increase of the Rct value over time. This data show already a high degree of specificity taking into consideration that they were obtained under extremely non-stringent conditions with the hybridisation taking place at room temperature far below the melting temperature of the probe/target complex and without any washing step involved after hybridisation. Hybridisation with a target, which only differs in one nucleotide in the middle of the target (SNP target), resulted in about 50% of target binding compared to the fully complementary target with a signal increase ratio obtained after 23 min hybridisation of four instead of eight from the fully complementary target.

Insert Scheme 1 and Figure 1 here

3.3 Electrochemical impedance spectroscopy tests performed at elevated temperatures

In order to perform biosensor measurements at various elevated temperatures all tests were performed in EIS measurement cells, which have been developed and produced in collaboration by MiniFAB Pty Ltd (Melbourne, Australia) as depicted in Figure 1. These measurement cells held the functionalised screen-printed electrodes between an aluminium metal base and a poly(methyl methacrylate) (PMMA) top layer. Both parts of the measurement cell were connected through two screws at the top and bottom end of the cell. Rubber O-rings around the electrode area held the solution within a reaction chamber on top of the electrodes and prevented solution leakage, as can be seen in Scheme 1 and in Figure S-1 of the Supporting Information. EIS buffer and target solution in EIS buffer were added through two holes in the PMMA layer below and above the three electrodes of the DropSens chip. These holes can also be fitted with tubing for pump-controlled flow through measurements. Electrical connection to the potentiostat was ensured through pogo pins, which attached to the connecting tracks of the electrode chips. The metal base ensured good heat transfer from heat blocks to the solution inside the measurement cell. This set-up was used to perform EIS measurements at different temperatures. To the best of our knowledge, this is the first example of kinetic EIS-based detection of nucleic acid targets performed at a range of different temperatures, which allowed the in-depth investigation of hybridisation and de-hybridisation kinetics at different temperatures. Figure 2 shows the EIS signal increase ratios, which were detected after 23 min hybridisation at a range of temperatures between 20 – 70 °C with the fully complementary *mcr-1* target, the *mcr-1* SNP target, a non-complementary target (NDM-7) (negative hybridisation control), and EIS buffer alone (negative EIS control), respectively. Figures S-2 and S-3 in the Supporting Information show the signal change ratios obtained at different hybridisation temperatures with p values at a 95% confidence interval. The data in Figure 2 and Table S3 in the Supporting Information show that there is basically no difference in the ratio of the signal increase ratio of the fully complementary target and the SNP target between 20 – 40 °C. At 50 °C, the signal increase ratio of the fully complementary target increased to 19. The value of the SNP target also

increased compared to the room temperature signal, but not as much as the fully complementary target, thus increasing the specificity of the target detection. The specificity is indicated here as the ratio of the signal increase ratio obtained from the perfect match (PM) target divided by the signal increase ratio of the SNP mismatch target (ratio (PM/MM(SNP)). The PM/MM ratio increased from 2.09 at 20 °C to 2.61 at 50 °C and then further to 3.42 at 60 °C, as can be seen in Table S3. A hybridisation temperature of 60 °C resulted in the biggest signal difference between the fully complementary target and the SNP target and thus the highest degree of specificity of the EIS-based *mcr-1* target detection, which could be achieved by means of an elevated hybridisation temperature. As can be seen in Figure 2, the increase in specificity is caused by a larger reduction of the signal of the SNP target than the signal from the fully complementary target. This indicates that a temperature of 60 °C was close to or above the melting temperature (T_m) of the SNP target/*mcr-1* probe duplex. Figure 2 also shows that the T_m of the fully complementary/*mcr-1* probe duplex was around 65 °C. At a temperature of 70 °C most of the fully complementary target was dissociated from the probe. The theoretical in-solution T_m value of the fully complementary/*mcr-1* duplex calculated with the Life Technologies PNA probe designer online tool was 80 °C for an oligonucleotide concentration of 1 µM, 71 °C for 1 nM, and 63 °C for 1 pM, respectively. The EIS biosensor tests in this study were performed with a target concentration of 1 µM. The T_m value of an oligonucleotide duplex in solution is increasing with increasing oligonucleotide concentration and is defined by the highest concentration of the two oligonucleotides that form the duplex [42]. In contrast to solution-based hybridisation, it is more complex to predict the melting temperature of surface bound DNA or PNA probes.[43–45] Ozel et al. e.g. found that the T_m values of surface-bound DNA probes were significantly lower than the predicted in-solution T_m values, which correlates with the results obtained in this study.[46]

Insert Figure 2 here

The temperature profiles of the EIS-based *mcr-1* target detection shown in Figure 2 does not follow the standard temperature profile of a solution based melt curve analysis, which usually shows a constant low signal below the melting temperature of the duplex, followed by a sigmoidal change around the T_m

value with a 50 % signal at the T_m value of the duplex.[45] In our case where the *mcr-1* PNA probe was immobilised on gold screen-printed electrodes via a self-assembled monolayer together with mercaptohexanol we observed a temperature profile which differed from the previously described solution temperature profile. The observed increase of the signal ratios of both the fully complementary and the SNP target at 50 °C is most likely related to an increase in the hybridisation efficiency and thus the amount of hybridised target at this temperature. One possible reason for this enhanced hybridisation efficiency is a rearrangement of the probe layer SAM on the gold electrode surface, which happened after the exposure of the SAM probe layer to this temperature. Such an enhanced hybridisation efficiency at elevated temperatures is a new phenomenon, which has, to the best of our knowledge, not been observed previously. Whereas, it has been shown that the solution temperature influences the structure of alkanethiol SAMs on gold surfaces. Yamada et al. showed that an increase of the solution temperature from -20 °C to 78 °C increased the size of well-ordered domains of decanethiol SAMs on gold surfaces and reduced the number of vacancy islands (pinholes), while increasing the size of these vacancy islands within the well-ordered SAM at higher temperatures.[47] Assuming a similar effect on the mixed monolayer of the *mcr-1* PNA probe with a terminal thiol group and mercaptohexanol, both, the increased size of well-ordered domains within the PNA/mercaptohexanol SAM and the larger size of pinholes within the SAM could be the cause of the observed increase in the hybridisation efficiency at 50 °C. The high surface roughness of screen-printed gold electrodes makes it very difficult if not impossible to perform similar optical analyses of the SAM that is formed on their surface with existing technologies, which usually require a very smooth surface.

3.4 De-hybridisation test

In order to further enhance the specificity of EIS biosensor measurements we used kinetic real-time EIS to investigate the de-hybridisation characteristics of fully complementary and single nucleotide mismatch targets at different temperatures. We chose 55 °C as this was the highest temperature where there was still significant SNP target binding and 60 °C, the temperature that allowed the highest level of SNP discrimination, and compared this with the behaviour at room temperature.

Figure 3, Figure 4, and Figure 5 show the hybridisation and de-hybridisation of fully complementary and single-nucleotide mismatch targets. The hybridisation towards the immobilised *mcr-1* PNA probe was followed for 23 min. Then the target solution was replaced by EIS buffer without target and the EIS measurement was continued for another 23 min to follow potential de-hybridisation of target molecules from the immobilised probes. Figure 3 shows that no de-binding of neither the fully complementary, nor the SNP target took place at room temperature. The Rct values stayed constant after the removal of the target solutions. As can be seen in Figure 4, a significant amount of the SNP target de-hybridised from the probe at 55 °C, whereas there was no de-binding the fully complementary target at this temperature. At 60 °C also the fully complementary target started to de-hybridise from the immobilised *mcr-1* PNA probe (see Figure 5). A signal reduction of about 20 % indicates that we are getting closer to the T_m value of the fully complementary/*mcr-1* probe duplex, but have not reached it yet as per definition there is a 50 % signal reduction at the melting temperature. These findings correlate well with the hybridisation temperature profile shown in Figure 2.

These data show that a combination of hybridisation and washing at elevated temperatures can even further enhance the specificity of EIS-based nucleic acid biosensors. A hybridisation and washing temperature of 55 °C further increased the PM/MM discrimination ratio to 5.7 by diminishing the mismatch signal during the wash step while keeping the perfect match signal.

Insert Figure 3, 4, and 5 here

3.5 Mcr-1 plasmid detection

We then applied the new *mcr-1* gene detection assay on *mcr-1* and NDM-1 *E. coli* reference strains to test the ability to specifically detect *mcr-1* gene harbouring bacterial plasmids. Figure 6 shows the successful direct detection of heat denatured *mcr-1* plasmids with the *mcr-1* specific PNA probe at 50 ^{0}C. Tests with *mcr-1* and NDM-1 plasmids showed that it was possible to detect the presence of *mcr-1* plasmids and to discriminate between these different plasmids carrying different resistance genes. Figure 6 RIGHT shows the Nyquist plot of an EIS measurement of a *mcr-1* probe functionalised

electrode before (red) and after 30 min hybridisation with 4 ng/μL heat denatured *mcr-1* plasmid (blue). All three baseline and seven EIS plots during target hybridisation with increasing charge transfer resistance values over time can be seen in Figure S-4 in the Supporting Information. The light blue lines represent the fitted data using the equivalent circuit model [$R_s([R_pW]Q)$] shown in the figure inset comprising of a solution resistance (R_s), the charge transfer resistance (R_p), a constant phase element and the Warburg impedance (W). Table S-4 shows example values of these circuit elements obtained from the fitting of an EIS spectrum with the above described equivalent circuit model. Measurements of the NDM-1 plasmid with *mcr-1* PNA functionalised electrodes and of *mcr-1* plasmid with our previously published NDM-specific PNA probe[39] as specificity control resulted in no signal increase beyond the buffer control signal. These data confirmed the high degree of specificity of our EIS-based *mcr-1* plasmid detection and demonstrate the capability of this new label-free molecular diagnostic test to detect *mcr-1* resistance genes in real bacterial samples.

Insert Figure 6 here

4 Conclusion

We have designed a set of *mcr-1* specific PNA probes for EIS-based colistin resistance *mcr-1* gene detection. A new flow cell enabled detailed kinetic binding and de-binding studies of perfect match and mismatched targets. This is to the best of our knowledge the first example of a temperature controlled kinetic EIS measurement. Optimal hybridisation and washing temperatures were determined to enhance the specificity of the newly designed *mcr-1* PNA probe. This is an important step towards the development of an EIS-based rapid, point-of-care molecular diagnostic test for AMR diagnosis to optimise patient treatment and reduce the miss-use of antibiotics.

Acknowledgements

The authors would like to thank Micah Atkin, MiniFAB Pty Ltd (Melbourne, Australia), for technical support during the project. The authors declare no conflict of interest.

Supporting Information for publication

Supporting information associated with this article can be found in the online version of this article at doi:

Table 1: *In-silico* analysis of newly designed *mcr-1* specific PNA probes and complementarity of these probes towards the *mcr-2* gene:

Rank	**CG%**	**PNA probe sequence**	**mcr-1 gene identity**	**Start position in *mcr-1***	**End position in *mcr-1***	**% purine (≤ 50%)**	**Purine stretch (≤ 4)**	***mcr-2* gene identity**	**mcr-1 PNA probe / *mcr-2* gene alignment**
1	50	gctcgttggcttagatgact	20/20 (100%)	1107	1126	45	3	16/20 (80%)	1101 GCTTGTCGGGCTAGATGACT 1120 |||.||.||..|||||||| 1 gctcgttggcttagatgact 20
2	40	caaggatctattaaacgcag	20/20 (100%)	351	370	60	5	16/24 (67%)	1326 AAGCATCGATTGGCTAAAAACGCA 1349 |||.|||.||| ||||||| 2 aaggatctatt------aaacgca 19
3	55	gaaagtctgggtgagaacgg	20/20 (100%)	1402	1421	75	5	14/17 (82%)	721 GTCGTCGGTGAG-ACGG 736 ||| |.||||| |||| 5 gtc-tgggtgagaacgg 20
4	35	aataattcggactcaaaagg	20/20 (100%)	982	1001	65	6	19/20 (95%)	976 AATAATTCAGACTCAAAAGG 995 ||||||||.||||||||||| 1 aataattcggactcaaaagg 20
5	55	tagtggtgttcgtcgtcggt	20/20 (100%)	716	735	45	2	20/20 (100%)	710 TAGTGGTGTTCGTCGTCGGT 729 |||||||||||||||||||| 1 tagtggtgttcgtcgtcggt 20
6	55	acaacgccatctgcaacacc	20/20 (100%)	1055	1074	45	2	17/20 (85%)	1049 ACAATACCATCTGTAACACC 1068 ||||..|||||||.|||||| 1 acaacgccatctgcaacacc 20

7	50	tggacggataagcaaactgg	20/20 (100%)	1489	1508	70	3	14/17 (82%)	999 GATGGATAAGCTACCTG 1015 ||.|||||||.|.||| 3 gacggataagcaaactg 19
8	50	ccagtttctttcgcgtgcat	20/20 (100%)	539	558	30	2	18/20 (90%)	533 CGAGTTTCTTTCGGGTGCAT 552 |.||||||||||.|||||| 1 ccagtttctttcgcgtgcat 20
9	40	tggcttttgttaaggtggat	20/20 (100%)	419	438	50	4	15/25 (60%)	142 GGCTTTATCATCTCAATGGCGGTGG 166 |||||| |.|.|| ||||| 2 ggcttt----tgttaa----ggtgg 18
10	55	gctcggtcagtccgtttgtt	20/20 (100%)	32	51	35	2	13/17 (77%)	31 TCTATCAATCCTTTTGT 47 ||..|||.|||.|||| 3 tcggtcagtccgtttgt 19

Figure captions:

Scheme 1: Principle of temperature enhanced *mcr-1* colistin resistance gene detection with EIS biosensors. (A) Faradaic label-free EIS detection of plasmid encoded resistance genes with sequence specific PNA probes attached to gold screen-printed electrodes in a mixed monolayer with mercaptohexanol with Ferri/Ferrocyanide ($K_4[Fe(CN)_6]$ + $K_3[Fe(CN)_6]$) as the redox active species in the solution. (B) Flow cell with aluminium base enabling temperature controlled kinetic EIS measurements (C). (D) Data analysis plotting charge transfer resistance values (Rct) over time.

Figure 1: LEFT: Kinetic EIS measurements of electrodes functionalised with *mcr-1* PNA probe 1 incubated with the mcr-1 fully complementary target, the mcr-1 target with one central miss-match, and with a non-complementary target (NDM-1), each at a concentration of 1 μM, as well as with EIS buffer as negative control. EIS measurements were performed at 20 °C. Target solutions were added at time 0 after three baseline EIS measurements with EIS buffer only. RIGHT: Signal increase ratios obtained after 23 min hybridisation with the different target solutions at 20 °C; significance was determined using ANOVA multiple comparison tests at a 95% confidence interval; * $p < 0.05$, ** $p < 0.01$, *** $p < 0.001$, **** $p < 0.0001$; data are presented as mean and standard deviation (SD); $n = 4$.

Figure 2: Average signal increase ratio detected with electrodes with functionalised *mcr-1* PNA probes after 23 min hybridisation with various 1 μM target solutions at different temperatures between 20 °C and 70 °C. The tested target solutions were the fully complementary *mcr-1* target (green), the mcr-1 SNP target (red), a non-complementary NDM target (orange), and EIS buffer alone (blue), respectively; data are presented as mean (SD); $n \geq 3$.

Figure 3: Hybridisation and de-hybridisation at 20°C. Average charge transfer resistance (R_{CT}) values before (time interval -10 min – 0) and after (time point 0) addition of 1 μM *mcr-1* fully complementary,

SNP target, and EIS buffer alone, respectively, at 20°C followed by replacement of the target solution with EIS buffer at time point 25 min and continued EIS measurements; data are presented as mean (SD); n =4.

Figure 4: Hybridisation and de-hybridisation at 55°C. Average R_{CT} values before (time interval -10 min – 0) and after (time point 0) addition of 1 μM *mcr-1* fully complementary, SNP target, and EIS buffer alone, respectively, at 55°C followed by replacement of the target solution with EIS buffer at time point 25 min and continued EIS measurements; data are presented as mean (SD); n =4.

Figure 5: Hybridisation and de-hybridisation at 60°C. Average R_{CT} values before (time interval -10 min – 0) and after (time point 0) addition of 1 μM *mcr-1* fully complementary, SNP target, and EIS buffer alone, respectively, at 60 °C followed by replacement of the target solution with EIS buffer at time point 25 min and continued EIS measurements; data are presented as mean (SD); n =4.

Figure 6: LEFT: Box and whiskers plot (min to max) of EIS-based *mcr-1* and NDM plasmid detection. The left part of the figure shows box plot data of signal increase ratios of *mcr-1* PNA functionalised electrodes after 30 min incubation with buffer only (buffer control, blue), 4 ng/μL heat denatured *mcr-1* plasmid (red), and 4 ng/μL heat denatured NDM plasmid (green), respectively. The right part shows box plot data of NDM specific PNA functionalised electrodes tested with the same targets (buffer control: blue; mcr-1 plasmid: red; NDM plasmid: green); n = 3. RIGHT: Nyquist plot EIS spectra of *mcr-1* PNA probe functionalised electrode before (red line and symbol) and after 30 min hybridisation with 4 ng/μL heat denatured *mcr-1* plasmid (dark blue line and symbol). The light blue lines show the fitted data using the equivalent circuit model shown in the figure inset with the solution resistance (Rs2), the charge transfer resistance (Rp2), the Warburg impedance and a constant phase element as components of the equivalent circuit.

Figures

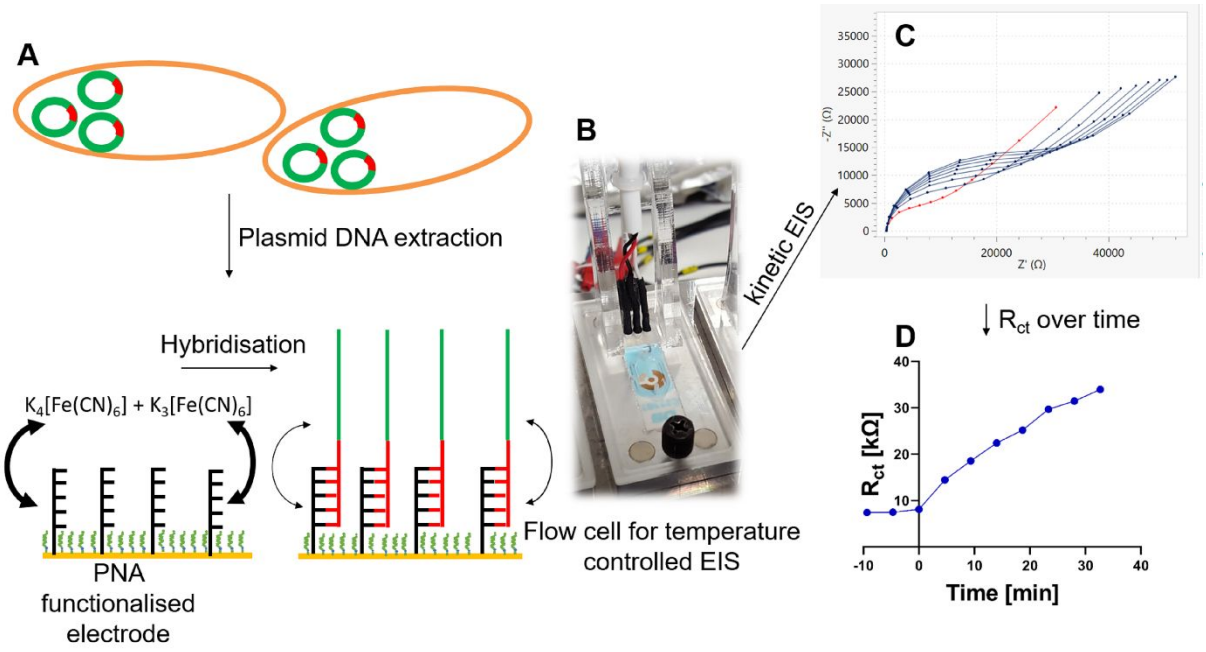

Scheme 1

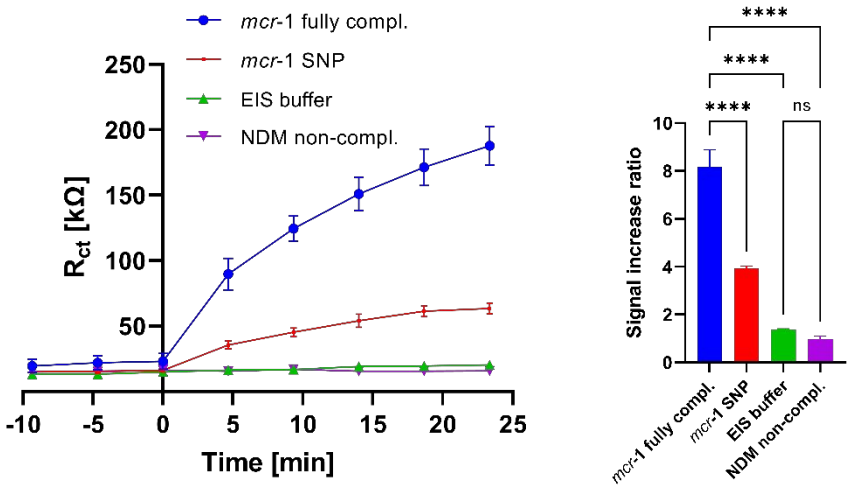
mcr-1 fully compl.
mcr-1 SNP
EIS buffer
NDM non-compl.
R_ct [kΩ]
250
200
150
100
50
-10
-5
0
5
10
15
20
25
Time [min]
****
****
****
ns
Signal increase ratio
10
8
6
4
2
0
mcr-1 fully compl.
mcr-1 SNP
EIS buffer
NDM non-compl.

Figure 1:

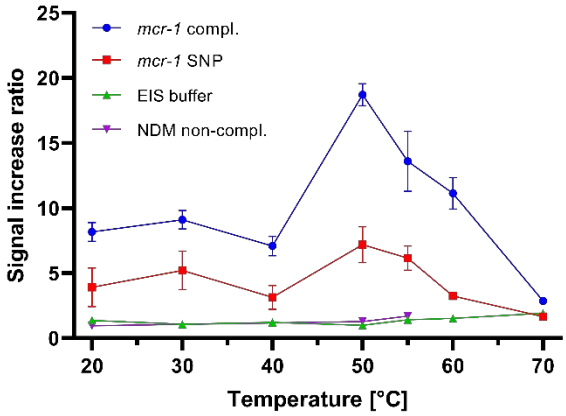
mcr-1 compl.
mcr-1 SNP
EIS buffer
NDM non-compl.
Signal increase ratio
Temperature [°C]
0
5
10
15
20
25
20
30
40
50
60
70

Figure 2:

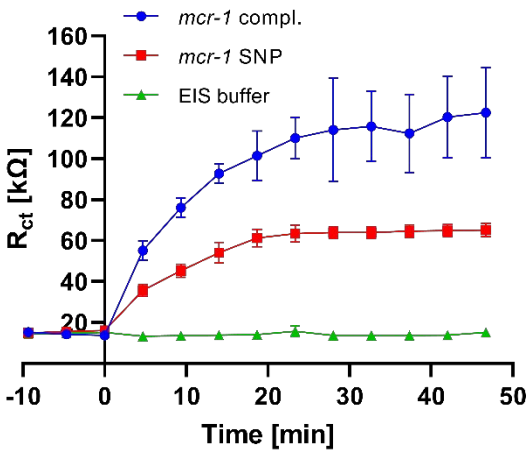
mcr-1 compl.
mcr-1 SNP
EIS buffer
160
140
120
100
80
60
40
20
R_{ct} [kΩ]
-10
0
10
20
30
40
50
Time [min]

Figure 3:

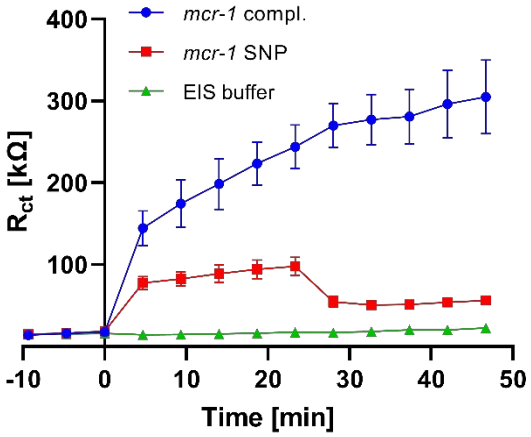
400
300
200
100
R_{ct} [kΩ]
-10
0
10
20
30
40
50
Time [min]
mcr-1 compl.
mcr-1 SNP
EIS buffer

Figure 4:

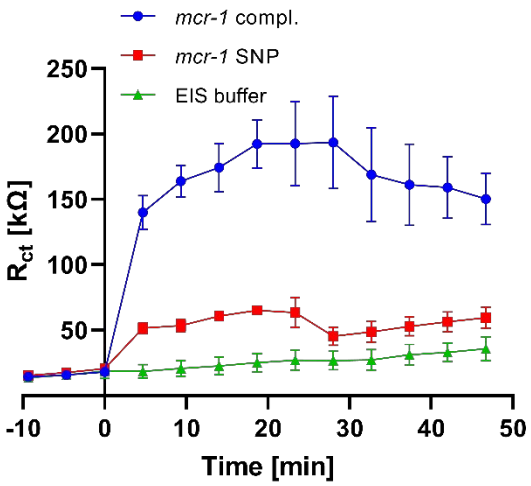
mcr-1 compl.
mcr-1 SNP
EIS buffer
250
200
150
100
50
R_ct [kΩ]
-10
0
10
20
30
40
50
Time [min]

Figure 5:

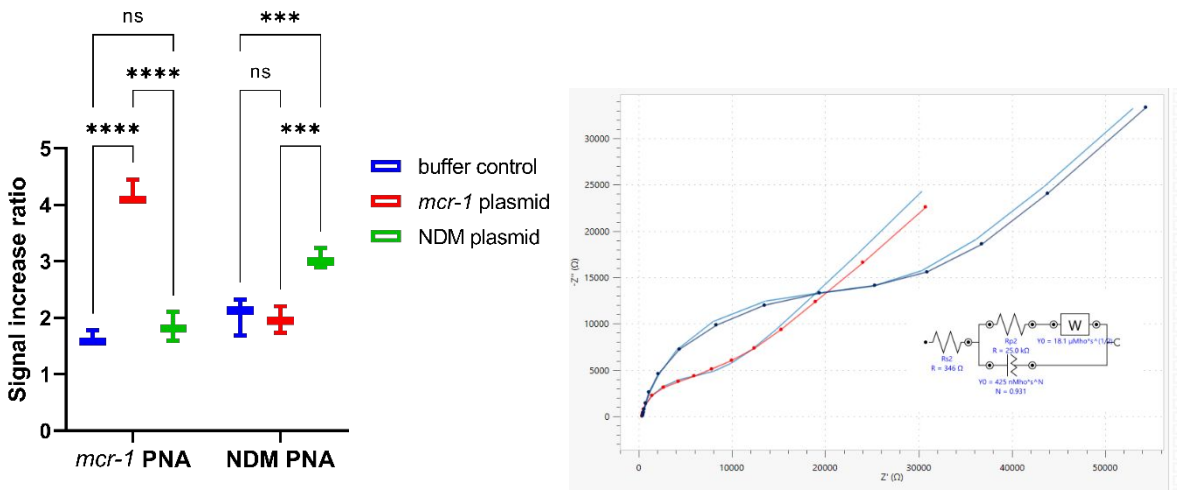
ns
***
****
ns
****
***
Signal increase ratio
0
1
2
3
4
5
mcr-1 PNA
NDM PNA
buffer control
mcr-1 plasmid
NDM plasmid
30000
25000
20000
15000
10000
5000
0
0
10000
20000
30000
40000
50000
W

Figure 6:

References

(1) The Review on Antimicrobial Resistance (Chaired by Jim O'Neill). *Tackling Drug-Resistant Infections Globally: Final Report and Recommendations*; 2016.

(2) Tacconelli E. and Margrini N. *Global Priority List of Antibiotic-Resistant Bacteria to Guide Research, Discovery, and Development of New Antibiotics.*; 2017.

(3) Baron, S.; Hadjadj, L.; Rolain, J. M.; Olaitan, A. O. Molecular Mechanisms of Polymyxin Resistance: Knowns and Unknowns. *Int. J. Antimicrob. Agents* **2016**, *48*, 583–591.

(4) Liu, Y. Y.; Wang, Y.; Walsh, T. R.; Yi, L. X.; Zhang, R.; Spencer, J.; Doi, Y.; Tian, G.; Dong, B.; Huang, X.; et al. Emergence of Plasmid-Mediated Colistin Resistance Mechanism MCR-1 in Animals and Human Beings in China: A Microbiological and Molecular Biological Study. *Lancet Infect. Dis.* **2016**, *16*, 161–168.

(5) Poirel, L.; Jayol, A.; Nordmanna, P. Polymyxins: Antibacterial Activity, Susceptibility Testing, and Resistance Mechanisms Encoded by Plasmids or Chromosomes. *Clinical Microbiology Reviews*. **2017**, pp 557–596.

(6) Falgenhauer, L.; Waezsada, S. E.; Yao, Y.; Imirzalioglu, C.; Käsbohrer, A.; Roesler, U.; Michael, G. B.; Schwarz, S.; Werner, G.; Kreienbrock, L.; et al. Colistin Resistance Gene Mcr-1 in Extended-Spectrum β-Lactamase-Producing and Carbapenemase-Producing Gram-Negative Bacteria in Germany. *Lancet Infect. Dis.* **2016**, *16*, 282–283.

(7) Yao, X.; Doi, Y.; Zeng, L.; Lv, L.; Liu, J. H. Carbapenem-Resistant and Colistin-Resistant Escherichia Coli Co-Producing NDM-9 and MCR-1. *Lancet Infect. Dis.* **2016**, *16*, 288–289.

(8) Kim, J.; Hwang, B. K.; Choi, H.; Wang, Y.; Choi, S. H.; Ryu, S.; Jeon, B. Characterization of Mcr-1-Harboring Plasmids from Pan Drug-Resistant Escherichia Coli Strains Isolated from Retail Raw Chicken in South Korea. *Microorganisms* **2019**, *7*, 6–13.

(9) Kaur, A.; Gandra, S.; Gupta, P.; Mehta, Y.; Laxminarayan, R.; Sengupta, S. Clinical Outcome of Dual Colistin- and Carbapenem-Resistant Klebsiella Pneumoniae Bloodstream Infections: A

Single-Center Retrospective Study of 75 Cases in India. *Am. J. Infect. Control* **2017**, *45*, 1289–1291.

(10) Zarkotou, O.; Pournaras, S.; Voulgari, E.; Chrysos, G.; Prekates, A.; Voutsinas, D.; Themeli-Digalaki, K.; Tsakris, A. Risk Factors and Outcomes Associated with Acquisition of Colistin-Resistant KPC-Producing Klebsiella Pneumoniae: A Matched Case-Control Study. *J. Clin. Microbiol.* **2010**, *48*, 2271–2274.

(11) Di Pilato, V.; Arena, F.; Tascini, C.; Cannatelli, A.; De Angelis, L. H.; Fortunato, S.; Giani, T.; Menichetti, F.; Rossolini, G. M. Mcr-1.2, a New Mcr Variant Carried on a Transferable Plasmid from a Colistin-Resistant KPC Carbapenemase-Producing Klebsiella Pneumoniae Strain of Sequence Type 512. *Antimicrob. Agents Chemother.* **2016**, *60*, 5612–5615.

(12) Lu, X.; Hu, Y.; Luo, M.; Zhou, H.; Wang, X.; Du, Y.; Li, Z.; Xu, J.; Zhu, B.; Xu, X.; et al. MCR-1.6, a New MCR Variant Carried by an IncP Plasmid in a Colistin-Resistant Salmonella Enterica Serovar Typhimurium Isolate from a Healthy Individual. **2017**, *61*, 6–10.

(13) Xavier, B. B.; Lammens, C.; Ruhal, R.; Kumar-Singh, S.; Butaye, P.; Goossens, H.; Malhotra-Kumar, S. Identification of a Novel Plasmid-Mediated Colistin- Resistance Gene , Mcr-2 , in Escherichia Coli , Belgium , June 2016. *Eurosurveillance* **2016**, *21*, 1–6.

(14) Yin, W.; Li, H.; Shen, Y.; Liu, Z.; Wang, S.; Shen, Z.; Zhang, R.; Walsh, T. R.; Shen, J.; Wang, Y. Novel Plasmid-Mediated Colistin Resistance Gene Mcr-3 in Escherichia Coli. *MBio* **2017**, *8*, 4–9.

(15) Wang, X.; Wang, Y.; Zhou, Y.; Li, J.; Yin, W.; Wang, S.; Zhang, S.; Shen, J.; Shen, Z.; Wang, Y. Emergence of a Novel Mobile Colistin Resistance Gene, Mcr-8, in NDM-Producing Klebsiella Pneumoniae Article. *Emerg. Microbes Infect.* **2018**, *7*, 1–9.

(16) Carroll, L. M.; Gaballa, A.; Guldimann, C.; Sullivan, G.; Henderson, L. O.; Wiedmanna, M. Identification of Novel Mobilized Colistin Resistance Gene Mcr- 9 in a Multidrug-Resistant, Colistin-Susceptible Salmonella Enterica Serotype Typhimurium Isolate. *MBio* **2019**, *10*, 1–6.

(17) Hays, J. P.; Mitsakakis, K.; Luz, S.; van Belkum, A.; Becker, K.; van den Bruel, A.; Harbarth, S.; Rex, J. H.; Simonsen, G. S.; Werner, G.; et al. The Successful Uptake and Sustainability of Rapid Infectious Disease and Antimicrobial Resistance Point-of-Care Testing Requires a Complex 'Mix-and-Match' Implementation Package. *Eur. J. Clin. Microbiol. Infect. Dis.* **2019**, *38*, 1015–1022.

(18) van Belkum, A.; Bachmann, T. T.; Lüdke, G.; Lisby, J. G.; Kahlmeter, G.; Mohess, A.; Becker, K.; Hays, J. P.; Woodford, N.; Mitsakakis, K.; et al. Developmental Roadmap for Antimicrobial Susceptibility Testing Systems. *Nat. Rev. Microbiol.* **2019**, *17*, 51–62.

(19) Hulme, J. Recent Advances in the Detection of Methicillin Resistant Staphylococcus Aureus (MRSA). *Biochip J.* **2017**, *11*, 89–100.

(20) Mach, K. E.; Wong, P. K.; Liao, J. C. Biosensor Diagnosis of Urinary Tract Infections: A Path to Better Treatment? *Trends Pharmacol. Sci.* **2011**, *32*, 330–336.

(21) McPartlin, D. A.; O'Kennedy, R. J. Point-of-Care Diagnostics, a Major Opportunity for Change in Traditional Diagnostic Approaches: Potential and Limitations. *Expert Rev. Mol. Diagn.* **2014**, *14*, 979–998.

(22) Scheler, O.; Glynn, B.; Kurg, A. Nucleic Acid Detection Technologies and Marker Molecules in Bacterial Diagnostics. *Expert Rev. Mol. Diagn.* **2014**, *14*, 489–500.

(23) Lam, B.; Fang, Z.; Sargent, E. H.; Kelley, S. O. Polymerase Chain Reaction-Free, Sample-to-Answer Bacterial Detection in 30 Minutes with Integrated Cell Lysis. *Anal. Chem.* **2012**, *84*, 21–25.

(24) Sin, M. L.; Mach, K. E.; Wong, P. K.; Liao, J. C. Advances and Challenges in Biosensor-Based Diagnosis of Infectious Diseases. *Expert Rev. Mol. Diagn.* **2014**, *14*, 225–244.

(25) Barreiros dos Santos, M.; Agusil, J. P.; Prieto-Simón, B.; Sporer, C.; Teixeira, V.; Samitier, J. Highly Sensitive Detection of Pathogen Escherichia Coli O157: H7 by Electrochemical Impedance Spectroscopy. *Biosens. Bioelectron.* **2013**, *45*, 174–180.

(26) Caygill, R. L.; Hodges, C. S.; Holmes, J. L.; Higson, S. P. J.; Blair, G. E.; Millner, P. A. Novel Impedimetric Immunosensor for the Detection and Quantitation of Adenovirus Using Reduced Antibody Fragments Immobilized onto a Conducting Copolymer Surface. *Biosens. Bioelectron.* **2012**, *32*, 104–110.

(27) Gebala, M.; Stoica, L.; Neugebauer, S.; Schuhmann, W. Label-Free Detection of DNA Hybridization in Presence of Intercalators Using Electrochemical Impedance Spectroscopy. *Electroanalysis* **2009**, *21*, 325–331.

(28) Gebala, M.; Schuhmann, W. Understanding Properties of Electrified Interfaces as a Prerequisite for Label-Free DNA Hybridization Detection. *Phys. Chem. Chem. Phys.* **2012**, *14*, 14933–14942.

(29) Ghindilis, A. L.; Smith, M. W.; Messing, D. S.; Haynes, V. N.; Middleton, G. B.; Schwarzkopf, K. R.; Campbell, C. E.; Zhan, C.; Ulrich, B.; Frasier, M. J.; et al. Development of Real-Time Assays for Impedance-Based Detection of Microbial Double-Stranded DNA Targets: Optimization and Data Analysis. *Biosens. Bioelectron.* **2012**, *35*, 87–93.

(30) Guo, X.; Kulkarni, A.; Doepke, A.; Halsall, H. B.; Iyer, S.; Heineman, W. R. Carbohydrate-Based Label-Free Detection of Escherichia Coli ORN 178 Using Electrochemical Impedance Spectroscopy. *Anal. Chem.* **2012**, *84*, 241–246.

(31) Jolly, P.; Tamboli, V.; Harniman, R. L.; Estrela, P.; Allender, C. J.; Bowen, J. L. Aptamer-MIP Hybrid Receptor for Highly Sensitive Electrochemical Detection of Prostate Specific Antigen. *Biosens. Bioelectron.* **2016**, *75*, 188–195.

(32) Riedel, M.; Kartchemnik, J.; Schöning, M. J.; Lisdat, F. Impedimetric DNA Detection-Steps Forward to Sensorial Application. *Anal. Chem.* **2014**, *86*, 7867–7874.

(33) Shin, S. R.; Zhang, Y. S.; Kim, D. J.; Manbohi, A.; Avci, H.; Silvestri, A.; Aleman, J.; Hu, N.; Kilic, T.; Keung, W.; et al. Aptamer-Based Microfluidic Electrochemical Biosensor for Monitoring Cell-Secreted Trace Cardiac Biomarkers. *Anal. Chem.* **2016**, *88*, 10019–10027.

(34) Tlili, C.; Sokullu, E.; Safavieh, M.; Tolba, M.; Ahmed, M. U.; Zourob, M. Bacteria Screening,

Viability, and Confirmation Assays Using Bacteriophage-Impedimetric/Loop-Mediated Isothermal Amplification Dual-Response Biosensors. *Anal. Chem.* **2013**, *85*, 4893–4901.

(35) Yang, Z.; Kasprzyk-Hordern, B.; Goggins, S.; Frost, C. G.; Estrela, P. A Novel Immobilization Strategy for Electrochemical Detection of Cancer Biomarkers: DNA-Directed Immobilization of Aptamer Sensors for Sensitive Detection of Prostate Specific Antigens. *Analyst* **2015**, *140*, 2628–2633.

(36) Henihan, G.; Schulze, H.; Corrigan, D. K.; Giraud, G.; Terry, J. G.; Hardie, A.; Campbell, C. J.; Walton, A. J.; Crain, J.; Pethig, R.; et al. Label- and Amplification-Free Electrochemical Detection of Bacterial Ribosomal RNA. *Biosens. Bioelectron.* **2016**, *81*, 487–494.

(37) Corrigan, D. K.; Schulze, H.; Henihan, G.; Hardie, A.; Ciani, I.; Giraud, G.; Terry, J. G.; Walton, A. J.; Pethig, R.; Ghazal, P.; et al. Development of a PCR-Free Electrochemical Point of Care Test for Clinical Detection of Methicillin Resistant Staphylococcus Aureus (MRSA). *Analyst* **2013**, *138*, 6997–7005.

(38) Corrigan, D. K.; Schulze, H.; Henihan, G.; Ciani, I.; Giraud, G.; Terry, J. G.; Walton, A. J.; Pethig, R.; Ghazal, P.; Crain, J.; et al. Impedimetric Detection of Single-Stranded PCR Products Derived from Methicillin Resistant Staphylococcus Aureus (MRSA) Isolates. *Biosens. Bioelectron.* **2012**, *34*, 178–184.

(39) Huang, J. M. Y.; Henihan, G.; Macdonald, D.; Michalowski, A.; Templeton, K.; Gibb, A. P.; Schulze, H.; Bachmann, T. T. Rapid Electrochemical Detection of New Delhi Metallo-Beta-Lactamase Genes To Enable Point-of-Care Testing of Carbapenem-Resistant Enterobacteriaceae. *Anal. Chem.* **2015**, *87*, 7738–7745.

(40) Ciani, I.; Schulze, H.; Corrigan, D. K.; Henihan, G.; Giraud, G.; Terry, J. G.; Walton, A. J.; Pethig, R.; Ghazal, P.; Crain, J.; et al. Development of Immunosensors for Direct Detection of Three Wound Infection Biomarkers at Point of Care Using Electrochemical Impedance Spectroscopy. *Biosens. Bioelectron.* **2012**, *31*, 413–418.

(41) Chen, S. H.; Lo, C. Z.; Su, S. Y.; Kuo, B. H.; Hsiung, C. A.; Lin, C. Y. UPS 2.0: Unique Probe Selector for Probe Design and Oligonucleotide Microarrays at the Pangenomic/ Genomic Level. *BMC Genomics* **2010**, *11* (SUPPL. 4), S6.

(42) Marky, L. A.; Breslauer, K. J. Calculating Thermodynamic Data for Transitions of Any Molecularity from Equilibrium Melting Curves. *Biopolymers* **1987**, *26*, 1601–1620.

(43) Allen, J. H.; Schoch, E. T.; Stubbs, J. M. Effect of Surface Binding on Heterogeneous DNA Melting Equilibria: A Monte Carlo Simulation Study. *J. Phys. Chem. B* **2011**, *115*, 1720–1726.

(44) Jayaraman, A.; Hall, C. K.; Genzer, J. Computer Simulation Study of Probe-Target Hybridization in Model DNA Microarrays: Effect of Probe Surface Density and Target Concentration. *J. Chem. Phys.* **2007**, *127* (14).

(45) Qiao, W.; Chiang, H. C.; Xie, H.; Levicky, R. Surface vs. Solution Hybridization: Effects of Salt, Temperature, and Probe Type. *Chem. Commun.* **2015**, *51*, 17245–17248.

(46) Ozel, A. B.; Srivannavit, O.; Rouillard, J. M.; Gulari, E. Target Concentration Dependence of DNA Melting Temperature on Oligonucleotide Microarrays. *Biotechnol. Prog.* **2012**, *28*, 556–566.

(47) Yamada, R.; Wano, H.; Uosaki, K. Effect of Temperature on Structure of the Self-Assembled Monolayer of Decanethiol on Au(111) Surface. *Langmuir* **2000**, *16*, 5523–5525.

For Table of Contents Only